Met O 11 Technical Note No 187

The Representation of Boundary Layer Turbulence in the Mesoscale Model: Part II - the scheme with changes of state

by

R. N. B. Smith

Forecasting Research Branch
Meteorological Office
London Road
Bracknell
Berkshire RG12 2SZ
United Kingdom

April 1984

FH2A

1. INTRODUCTION

Technical Note No 186[1] described a representation of turbulence based on a $1\frac{1}{2}$-order closure of the hierarchy of equations for turbulent correlations. The scheme was dry in that it took no account of water vapour/liquid water changes of state. A more accurate description of the scheme would be "moist" since the effect of water vapour on buoyancy was represented through the use of virtual potential temperature. This note describes the modifications necessary to make the scheme "wet", i.e. to take account of vapour/liquid state changes on both the resolved and turbulent eddy scales.

The effects of these changes of state on turbulent transport are most easily represented by using thermodynamic and water content variables conserved during the phase changes. (The term "conservative" will be used in this note to mean "conserved during vapour/liquid phase changes). These new variables are introduced in § 2. The usual, but non-conservative variables, potential temperature (θ), specific humidity (q) and specific liquid water content (q_l) are still required to calculate buoyancy forces (through the virtual potential temperature $\theta_v = \theta(1 + 0.608q - q_l)$), radiative effects (dependent on $T = \pi\theta$) and precipitation physics (dependent on q_l and q). θ, q and q_l have to be diagnosed from the conservative variables using cloud ensemble relations which are discussed in § 3.

2. THE USE OF CONSERVATIVE VARIABLES

2.1 The conservative variables

The use of variables conserved during phase changes eliminates the need to consider source/sink terms due to the changes in prognostic equations. Such terms can be dealt with satisfactorally in the equations for the mean variables by well established grid-scale parametrizations (Machin (1983)).

---

1 hereafter referred to as (I)

However, it is not so simple to treat the fluctuations in the phase changes due to turbulence. Working with conservative variables in the equations for turbulent correlations simplifies the analysis.

The conservative water variable is the specific total water content defined as the sum of the specific humidity and the specific liquid water content:

$$q_t \equiv q + q_l \qquad (2.1.1)$$

q_t satisfies the equation

$$\frac{Dq_t}{Dt} = -\frac{1}{\rho}\frac{\partial}{\partial z}\left(\rho \overline{w'q_t'}\right) + F_{q_t} \qquad (2.1.2)$$

in the absence of precipitation and cloud water settling. The conserved thermodynamic variable to be used is the liquid water potential temperature θ_l defined by

$$c_p \frac{d\theta_l}{\theta_l} \equiv c_p \frac{d\theta}{\theta} - d\left(\frac{L q_l}{T}\right) = \frac{dQ}{T} \qquad (2.1.3)$$

From this definition it can be deduced that

$$\theta_l = \theta \exp\left(-\frac{L q_l}{c_p T}\right) \qquad (2.1.4)$$

or $$\theta_l \simeq \theta - \frac{L q_l}{c_p \pi} \qquad (2.1.5)$$

since $L q_l / c_p T \sim 0 - 10^{-2} \ll 1$ if $q_l \sim 0 - 10^{-3}$ kg kg^{-1}. Also, from the definition it follows that

$$\frac{D\theta_l}{Dt} = -\frac{1}{\rho}\frac{\partial}{\partial z}\left(\rho \overline{w'\theta_l'}\right) + \frac{R}{c_p \pi} + F_{\theta_l} \qquad (2.1.6)$$

upon making the assumption that $L q_l / c_p T$ can be neglected relative to unity. In (2.1.2) and (2.1.6) F_{q_t} and F_{θ_l} represent horizontal diffusion terms and R is the radiative flux divergence. The forms of equations (2.1.2) and (2.1.6) are identical to those of the equations they replace i.e. I(2.1.3) and I(2.1.2) respectively.

The turbulence parametrization problem is now shifted to finding representations of the vertical fluxes $\overline{w' \underline{v}_H'}$, $\overline{w' \theta_l'}$ and $\overline{w' q_t'}$ in terms of the mean variables $\underline{v}$, θ_l and q_t and the t.k.e. $\bar{E}$.

2.2 The modified equations for turbulent correlations

The equations for the second order turbulent correlations are the same as I(2.3.1)-(2.3.12) except that in I(2.3.2)-(2.3.8) θ is replaced by θ_l and q by q_t so that:

$$\overline{w' \theta_l'} = \tau_2 \left[-\overline{w'^2} \frac{\partial \theta_l}{\partial z} + (1 - a_2) \frac{g}{\theta_v} \overline{\theta_v' \theta_l'} \right] \qquad (2.2.1)$$

$$\overline{w' q_t'} = \tau_2 \left[-\overline{w'^2} \frac{\partial q_t}{\partial z} + (1 - a_2) \frac{g}{\theta_v} \overline{\theta_v' q_t'} \right] \qquad (2.2.2)$$

$$\overline{\underline{v}_H' \theta_l'} = -\tau_2 \left[\overline{w' \underline{v}_H'} \frac{\partial \theta_l}{\partial z} + (1 - a_2) \overline{w' \theta_l'} \frac{\partial \underline{v}_H}{\partial z} \right] \qquad (2.2.3)$$

$$\overline{\underline{v}_H' q_t'} = -\tau_2 \left[\overline{w' \underline{v}_H'} \frac{\partial q_t}{\partial z} + (1 - a_2) \overline{w' q_t'} \frac{\partial \underline{v}_H}{\partial z} \right] \qquad (2.2.4)$$

$$\overline{\theta_l'^2} = -2 \tau_3 \overline{w' \theta_l'} \frac{\partial \theta_l}{\partial z} \qquad (2.2.5)$$

$$\overline{q_t'^2} = -2 \tau_3 \overline{w' q_t'} \frac{\partial q_t}{\partial z} \qquad (2.2.6)$$

$$\overline{\theta_l' q_t'} = -\tau_3 \left[\overline{w' \theta_l'} \frac{\partial q_t}{\partial z} + \overline{w' q_t'} \frac{\partial \theta_l}{\partial z} \right] \qquad (2.2.7)$$

The virtual potential temperature in the presence of liquid water becomes

$$\theta_v = \theta(1 + \delta q - q_l) \qquad (2.2.8)$$

where $\delta = 1/\varepsilon - 1$ and $\varepsilon = 0.622$, $\delta = 0.608$. In place of I(2.3.13) we therefore have

$$\frac{g}{\theta_v}\theta_v' = \beta_T \theta_l' + \beta_w q_t' + \beta_L q_l' \qquad (2.2.9)$$

where the buoyancy parameters are:

$$\beta_T = \frac{g}{\theta}, \quad \beta_w = \frac{g\delta}{(1+\delta q - q_l)}, \quad \beta_L = \frac{L}{c_p \pi}\beta_T - \frac{\beta_w}{\eta} \qquad (2.2.10)$$

$\eta = 1 - \varepsilon = 0.378$.

Unlike the dry or moist case we no longer have a closed set of equations for the turbulent correlations since (2.2.9) and (2.2.10) involve q_l and q_l' in addition to the conserved variables. Relationships between q_l and q_l' and the conserved quantities have to be found by considering cloud ensembles and their temperature and humidity statistics. Some precise forms of these relationships will be derived in the next section; here we will write the general forms:

$$q_l = q_l(p, \theta_l, q_t, \overline{\theta_l'^2}, \overline{\theta_l' q_t'}, \overline{q_t'^2}, \text{possibly higher order correlations}) \qquad (2.2.11)$$

$$\theta = \theta(p, \theta_l, q_t, \overline{\theta_l'^2}, \overline{\theta_l' q_t'}, \overline{q_t'^2}, \ldots\ldots\ldots) \qquad (2.2.12)$$
$$= \theta_l - \frac{L}{c_p \pi} q_l$$

$$q = q(p, \theta_l, q_t, \overline{\theta_l'^2}, \overline{\theta_l' q_t'}, \overline{q_t'^2}, \ldots\ldots\ldots) \qquad (2.2.13)$$
$$= q_t - q_l$$

$$\theta_v = \theta(1 + \delta q - q_l) \qquad (2.2.14)$$

for the mean variables and:

$$\frac{g}{\theta_v}\overline{\theta_v'\phi'} = \bar{\beta}_T\left(p, \theta_l, q_t, \overline{\theta_l'^2}, \ldots\right)\overline{\theta_l'\phi'} + \bar{\beta}_w\left(p, \theta_l, q_t, \overline{\theta_l'^2}, \ldots\right)\overline{q_t'\phi'} \qquad (2.2.15)$$

for second order correlations involving θ_v' and any other conservative variable ϕ . In the absence of any cloud (2.2.11) - (2.2.15) must become

$$q_l = 0$$

$$q = q_t$$

$$\theta_v = \theta\left(1 + \delta q\right)$$

$$\frac{g}{\theta_v}\overline{\theta_v'\phi'} = \beta_T\,\overline{\theta'\phi'} + \beta_w\,\overline{q'\phi'} \qquad \text{(cf. equation I(2.3.13))}$$

Comparison of (2.2.15) with I(2.3.13) shows that the formalism in (I) goes through unchanged provided $\theta \rightarrow \theta_l$, $q \rightarrow q_t$, $\beta_T \rightarrow \bar{\beta}_T$ and $\beta_w \rightarrow \bar{\beta}_w$. Thus we have

$$\overline{w'\theta_l'} = -K_h\frac{\partial \theta_l}{\partial z} \qquad (2.2.16)$$

$$\overline{w'q_t'} = -K_h\frac{\partial q_t}{\partial z} \qquad (2.2.17)$$

$$\overline{w'\underline{v}_H'} = -K_m\frac{\partial \underline{v}_H}{\partial z} \qquad (2.2.18)$$

with K_h, K_m given by I(2.4.6) and I(2.4.7) and N^2 given by:

$$N^2 = \bar{\beta}_T\frac{\partial \theta_l}{\partial z} + \bar{\beta}_w\frac{\partial q_t}{\partial z} \qquad (2.2.19)$$

If it is also assumed that:

$$\frac{g}{\theta_v}\overline{\theta_v'\phi'\psi'} = \bar{\beta}_T\,\overline{\theta_l'\phi'\psi'} + \bar{\beta}_w\,\overline{q_t'\phi'\psi'} \qquad (2.2.20)$$

for third order turbulent correlations involving θ_v' and any conservative variables ϕ and ψ the formalism in I§2.8 for third order correlations remains the same but again with $\theta \rightarrow \theta_L$, $q \rightarrow q_t$, $\beta_T \rightarrow \bar{\beta}_T$ and $\beta_w \rightarrow \bar{\beta}_w$. Thus:

$$\overline{w'\bar{E}} = -K_E \frac{\partial \bar{E}}{\partial z} - K_2 g_2 - K_3 g_3 \qquad (2.2.21)$$

$$g_2 = \bar{\beta}_T \frac{\partial}{\partial z}\left(\overline{w'\theta_L'}\right) + \bar{\beta}_w \frac{\partial}{\partial z}\left(\overline{w'q_t'}\right) \qquad (2.2.22)$$

$$g_3 = \bar{\beta}_T^{\,2} \frac{\partial \overline{\theta_L'^2}}{\partial z} + 2\bar{\beta}_T \bar{\beta}_w \frac{\partial\left(\overline{\theta_L' q_t'}\right)}{\partial z} + \bar{\beta}_w^{\,2} \frac{\partial \overline{q_t'^2}}{\partial z} \qquad (2.2.23)$$

with K_E, K_2 and K_3 given by I(2.8.9) - (2.8.11) and N^2 by (2.2.19).

2.3 Surface layer stability and fluxes in terms of conservative variables

The existing parametrization of surface turbulence fluxes in based on the following similarity laws which are valid in the absence of changes of state:

$$\frac{\partial u}{\partial z} = \frac{u_*}{kz}\varphi_m\left(\frac{z}{L}\right) \qquad (2.3.1)$$

$$\frac{\partial \theta}{\partial z} = \frac{\theta_*}{kz}\varphi_h\left(\frac{z}{L}\right) \qquad (2.3.2)$$

$$\frac{\partial q}{\partial z} = \frac{q_*}{kz}\varphi_h\left(\frac{z}{L}\right) \qquad (2.3.3)$$

where

$$u_* = \left|\left(\overline{w'\underline{v}_H'}\right)_{surf}\right|^{1/2}$$

$$\theta_* = -\left(\overline{w'\theta'}\right)_{surf} / u_*$$

$$q_* = -\left(\overline{w'q'}\right)_{surf} / u_*$$

and the Monin-Obukov length $L = u_*^2 / k B_*$

with

$$B_* = \frac{-g}{\theta_{v1}} \frac{(\overline{w'\theta_v'})_{surf}}{u_*} = \beta_{T1}\,\theta_* + \beta_{w1}\,q_* \quad , \quad \beta_{T1} = \frac{g}{\theta_1} \quad , \quad \beta_{w1} = \frac{g\delta}{(1+\delta q_1)} \, .$$

From these similarity laws and the assumption that the fluxes are approximately constant in the surface layer it is deduced that the surface fluxes are given by:

$$(\overline{w'\underline{v}_H'})_{surf} = -C_D\left(Ri_b, \log z_1/z_0\right)|\underline{v}_1|\,\underline{v}_1 \qquad (2.3.4)$$

$$(\overline{w'\theta'})_{surf} = -C_H\left(Ri_b, \log z_1/z_0\right)|\underline{v}_1|\,(\theta_1 - \theta_{surf}) \qquad (2.3.5)$$

$$(\overline{w'q'})_{surf} = -C_H\left(Ri_b, \log z_1/z_0\right)|\underline{v}_1|\,\alpha\left(q_1 - q_{sat}(T_{surf})\right) \qquad (2.3.6)$$

where $\alpha = 1/(1 + C_H|\underline{v}_1|r_s)$, r_s is the surface resistance to evaporation,

$$Ri_b = N_{surf}^2 / S_{surf}^2$$

$$N_{surf}^2 = \beta_{T1}\frac{(\theta_1 - \theta_{surf})}{z_1} + \beta_{w1}\,\alpha\,\frac{(q_1 - q_{sat}(T_{surf}))}{z_1} \qquad (2.3.7)$$

$$S_{surf}^2 = |\underline{v}_1|^2 / z_1^2 \qquad (2.3.8)$$

The total, ie. sensible + latent, heat flux into the atmosphere is required in the surface energy budget calculations. It is given by

$$\mathcal{H} = H + LE = \rho c_p \pi_{surf}(\overline{w'\theta'})_{surf} + \rho L(\overline{w'q'})_{surf}$$

$$= \rho c_p \pi_{surf}\left[(\overline{w'\theta'})_{surf} + \frac{L}{c_p \pi_{surf}}(\overline{w'q'})_{surf}\right] \qquad (2.3.9)$$

By the same reasoning which lead to the modifications to the turbulence scheme above the surface layer, the "wet" surface layer scheme is obtained by making the substitutions $\theta \rightarrow \theta_l$, $q \rightarrow q_t$, $\beta_T \rightarrow \bar{\beta}_T$, $\beta_w \rightarrow \bar{\beta}_w$. Thus the similarity laws valid with changes of state can be written in terms of conservative variables as:

$$\frac{\partial u}{\partial z} = \frac{u_*}{kz} \varphi_m \left(\frac{z}{L}\right) \qquad (2.3.10)$$

$$\frac{\partial \theta_l}{\partial z} = \frac{\theta_{l*}}{kz} \varphi_h \left(\frac{z}{L}\right) \qquad (2.3.11)$$

$$\frac{\partial q_t}{\partial z} = \frac{q_{t*}}{kz} \varphi_h \left(\frac{z}{L}\right) \qquad (2.3.12)$$

where the scaling parameters are defined by

$$u_* = \left| \left(\overline{w' \underline{v}_H'}\right)_{surf} \right|^{1/2}$$

$$\theta_{l*} = -\left(\overline{w' \theta_l'}\right)_{surf} / u_*$$

$$q_{t*} = -\left(\overline{w' q_t'}\right)_{surf} / u_*$$

The Monin-Obukov length is still given by $L = u_*^2 / k B_*$ but the scaling parameter for buoyancy is now given by

$$B_* = \bar{\beta}_{T1} \theta_l^* + \bar{\beta}_{w1} q_t^*$$

The surface fluxes are:

$$\left(\overline{w' \underline{v}_H'}\right)_{surf} = -c_D \left(Ri_b, \log z_1/z_0\right) |\underline{v}_1| \underline{v}_1 \qquad (2.3.13)$$

$$\left(\overline{w' \theta_l'}\right)_{surf} = -c_H \left(Ri_b, \log z_1/z_0\right) |\underline{v}_1| \left(\theta_{l1} - \theta_{surf}\right) \qquad (2.3.14)$$

$$(\overline{w'q_t'})_{surf} = -c_H(Ri_b, \log z_1/z_0)|\underline{v}_1| \propto (q_{t1} - q_{sat}(T_{surf})) \quad (2.3.15)$$

with the surface bulk Richardson number Ri_b calculated with

$$N^2_{surf} = \overline{\beta}_{T1}\frac{(\theta_{l1} - \theta_{surf})}{z_1} + \overline{\beta}_{w1} \propto \frac{(q_{t1} - q_{sat}(T_{surf}))}{z_1} \quad (2.3.16)$$

Equation (2.3.9) can be rewritten as

$$\mathcal{H} = \rho c_p \Pi_{surf}\left[(\overline{w'\theta_l'})_{surf} + \frac{L}{c_p \Pi_{surf}}(\overline{w'q_t'})_{surf}\right]$$

$$= \rho c_p \Pi_{surf}(\overline{w'\theta_l'}) + \rho L (\overline{w'q_t'})_{surf} \quad (2.3.17)$$

retaining the form of (2.3.9a). It is not permissible to identify the two terms in (2.3.17) as the sensible and latent heat components as in the moist case unless

$$(\overline{w'q_l'})_{surf} \ll (\overline{w'q'})_{surf} \quad \text{and} \quad \frac{L}{c_p \Pi_{surf}}(\overline{w'q_l'})_{surf} \ll (\overline{w'\theta'})_{surf}.$$

3. CLOUD ENSEMBLE RELATIONS

3.1 The determination of ensemble mean cloud fraction, liquid water content and buoyancy parameters

In reality a given fluid element in the atmosphere at a given time is in a state of saturation or not. However, due to turbulent fluctuations in temperature and humidity, this state is liable to change. After an ensemble average is taken a partial cloudiness may result. In accordance with the assumption of (I) that ensemble means are identified with horizontal means over a grid-box, the ensemble mean cloud fraction is taken to represent the fractional cloud cover. The aim of this section is to derive expressions for the mean cloud fraction and other quantities dependent on the ensemble statistics. The approach to be used is that developed by Sommeria and Deardorff (1977) and Mellor (1977).

In order to find the liquid water content of a fluid element with given θ_l and q_t an expression $\tilde{q}_s(\theta_l, q_t, p)$ is required for the saturation specific humidity. From the definitions of θ_l and q_t :

$$\tilde{q}_s(\theta_l, q_t, p) = q_s\left(T_l + \frac{L}{c_p}(q_t - q_s), p\right)$$

where $T_l = \pi\theta_l$ and $q_s(T,p)$ is the saturation specific humidity curve. An approximation based on the assumption that $Lq_l/c_pT_l \ll 1$ (see (2.1.5)) is

$$\tilde{q}_s(\theta_l, q_t, p) = q_s(T_l, p) + \left.\frac{\partial q_s}{\partial T}\right|_{T=T_l} \cdot \frac{L}{c_p}\left(q_t - \tilde{q}_s(\theta_l, q_t, p)\right)$$

which can be rewritten as

$$\tilde{q}_s(\theta_l, q_t, p) = \frac{(1+\gamma_l q_t) q_{sl}}{(1+\gamma_l q_{sl})} \qquad (3.1.1)$$

where $q_{sl} \equiv q_s(T_l, p) = \frac{\varepsilon e_{sl}}{(p - \eta e_{sl})}$, $\eta = 1-\varepsilon$, $e_{sl} = e_{sat}(T_l)$

$$\gamma_l = \frac{L}{c_p}\alpha_l \quad , \quad \alpha_l = \left.\frac{\partial q_s}{\partial T}\right|_{T=T_l} = \frac{\varepsilon L q_{sl}}{R T_l^2} \cdot \frac{p}{(p - \eta e_{sl})} .$$

The last relation follows from the Clausius-Clapeyron equation

$$\frac{de_s}{dT} = \frac{\varepsilon L e_s}{RT^2}$$

Now if $q_t \leq \tilde{q}_s(\theta_l, q_t, p)$ then $q_l = 0$, $q = q_t$ and $\theta = \theta_l$ otherwise (ie if $q_t > \tilde{q}_s(\theta_l, q_t, p)$)

$$q_l = q_t - \tilde{q}_s(\theta_l, q_t, p) = \frac{(q_t - q_{sl})}{(1+\gamma_l q_{sl})} \qquad (3.1.2)$$

$$q = \tilde{q}_s(\theta_l, q_t, p)$$

$$\theta = \theta_l + \frac{L}{c_p \pi} q_l$$

Now introducing the ensemble mean of a quantity (denoted by an overbar) and a turbulent fluctuation from the mean (denoted by a prime) we write

$$q_t = \bar{q}_t + q_t' \quad \text{and} \quad \theta_l = \bar{\theta}_l + \theta_l'$$

Then

$$q_{sl} \simeq \bar{q}_{sl} + \bar{b}_l \theta_l' \quad \text{where} \quad \bar{q}_{sl} = q_s(\bar{T}_l, \bar{p}), \quad \bar{b}_l = \Pi \bar{\alpha}_l, \quad \bar{\alpha}_l = \left.\frac{\partial q_s}{\partial T}\right|_{T=\bar{T}_l}$$

So

$$q_l \simeq \frac{\bar{q}_t + q_t' - \bar{q}_{sl} - \bar{b}_l \theta_l'}{(1 + \bar{\delta}_l \bar{q}_{sl})} = \bar{a}_l (\bar{q}_t - \bar{q}_{sl}) + s' \qquad (3.1.3)$$

when $s' > -\bar{a}_l (\bar{q}_t - \bar{q}_{sl})$,

and $q_l = 0$ when $s' \leq -\bar{a}_l (\bar{q}_t - \bar{q}_{sl})$

where $\bar{a}_l = 1/(1 + \bar{\delta}_l \bar{q}_{sl})$ and $s' = \bar{a}_l (q_t' - \bar{b}_l \theta_l')$ (3.1.4).

It is convenient to normalise s' and $\bar{a}_l (\bar{q}_t - \bar{q}_{sl})$ with the standard deviation

$$\sigma_s \equiv (\overline{s'^2})^{1/2} = \bar{a}_l \left(\overline{q_t'^2} - 2\bar{b}_l \overline{q_t' \theta_l'} + \bar{b}_l^2 \overline{\theta_l'^2} \right) \qquad (3.1.5)$$

and write

$$t = s'/\sigma_s \quad \text{and} \quad Q_1 = \bar{a}_l (\bar{q}_t - \bar{q}_{sl})/\sigma_s$$

Equation (3.1.3) can then be written as

$$\frac{q_l}{\sigma_s} = \begin{cases} Q_1 + t & t > -Q_1 \\ 0 & t \leq -Q_1 \end{cases} \qquad (3.1.6)$$

In order to determine ensemble means of non-conservative quantities a probability distribution function (p.d.f.) G(t) has to be introduced. From the definition of a p.d.f. G must satisfy

$$\int_{-\infty}^{\infty} G(t)\,dt = 1 \qquad (3.1.7)$$

Now $\overline{s'} = \bar{a}_c\left(\overline{q_t'} - \bar{b}_c\,\overline{\theta_l'}\right) = 0$ and so

$$\int_{-\infty}^{\infty} t\,G(t)\,dt = 0 \qquad (3.1.8)$$

Also we know $$\int_{-\infty}^{\infty} t^2 G(t)\,dt = \frac{\overline{s'^2}}{\sigma_s^2} = 1 \qquad (3.1.9)$$

The ensemble mean cloud fraction C is defined as the proportion of ensemble members having a liquid water content greater than zero:

$$C = \int_{-Q_1}^{\infty} G(t)\,dt \qquad (3.1.10)$$

The ensemble mean specific liquid water content $\bar{q}_l$ is given by

$$\frac{\bar{q}_l}{\sigma_s} = \int_{-Q_1}^{\infty} (Q_1 + t)\,G(t)\,dt = C Q_1 + \int_{-Q_1}^{\infty} t\,G(t)\,dt \qquad (3.1.11)$$

It should be noted that the mean value of q_l in cloud is $\bar{q}_l/C$ in the sense that

$$\bar{q}_l = (1-C)*0 + C*\frac{\bar{q}_l}{C}$$

In the same sense

$$q = \begin{cases} \bar{q}_t \\ \bar{q}_t - \bar{q}_l/C \end{cases}, \quad \theta = \begin{cases} \bar{\theta}_l & \text{outside cloud} \\ \bar{\theta}_l + \frac{L}{c_p \Pi}\frac{\bar{q}_l}{C} & \text{in cloud} \end{cases};$$

then

$$\bar{q} = (1-C)\bar{q}_t + C\left(\bar{q}_t - \bar{q}_l/C\right) = \bar{q}_t - \bar{q}_l$$

$$\bar{\theta} = (1-C)\bar{\theta}_l + C\left(\bar{\theta}_l + \frac{L}{c_p \Pi}\frac{\bar{q}_l}{C}\right) = \bar{\theta}_l + \frac{L}{c_p \Pi}\bar{q}_l \,.$$

When calculating precipitation and radiative fluxes in cloud it is the in-cloud mean values which should be used. The grid-box mean precipitation and radiative fluxes are then C times the values calculated. Unless the processes are linear this will not be the same as the result from calculations using $\bar{q}$, $\bar{q}_l$ and $\bar{\theta}$.

The deviation from ensemble mean liquid water content, q_l', is given by:

$$\frac{q_l'}{\sigma_s} = \begin{cases} Q_1 + t - \bar{q}_l/\sigma_s & t > -Q_1 \\ -\bar{q}_l/\sigma_s & t \leq -Q_1 \end{cases} \qquad (3.1.12)$$

from which it is easily verified that $\overline{q_l'} = \int_{-\infty}^{\infty} q_l'(t)\, G(t)\, dt = 0$.

It is stated as a hypothesis by Bougeault (1982) that

$$\overline{\phi' q_l'} = \overline{\phi' s'}\left(\overline{s' q_l'}/\sigma_s^2\right) = \bar{a}_l R\left(\overline{\phi' q_l'} - \bar{b}_l \overline{\phi' \theta_l'}\right) \qquad (3.1.13)$$

where $R = \left(\overline{s' q_l'}/\sigma_s^2\right)$ for any conservative quantity ϕ, whatever the form of G(t). Mellor (1977) proves that this is true for a normal distribution. However, for this special case it can be shown that R=C. So

$$\overline{\phi' q_l'} = C\left(\overline{\phi' s'}\right) = \bar{a}_l C\left(\overline{\phi' q_l'} - \bar{b}_l \overline{\phi' \theta_l'}\right) \qquad (3.1.13a)$$

may be an alternative generalisation to (3.1.13). The quantity R can be evaluated as an integral involving G:

$$R = \int_{-\infty}^{\infty} t\, \frac{q_l'(t)}{\sigma_s}\, G(t)\, dt = -\frac{\bar{q}_l}{\sigma_s}\int_{-\infty}^{\infty} t\, G(t)\, dt + \int_{-Q_1}^{\infty} t\,(Q_1 + t)\, G(t)\, dt$$

$$= \int_{-Q_1}^{\infty} t\,(Q_1 + t)\, G(t)\, dt \qquad (3.1.14)$$

From (3.1.8) and (3.1.9) it can be seen that $R \to 1$ as $C \to 1$. Equations (2.2.9) and (3.1.13) give

$$\frac{g}{\theta_v}\overline{\theta_v' \phi'} = \beta_T \overline{\theta_l' \phi'} + \beta_w \overline{q_t' \phi'} + \beta_L \overline{q_l' \phi'}$$

$$= \left(\beta_T - \bar{a}_l \bar{b}_l R \beta_L\right)\overline{\theta_l' \phi'} + \left(\beta_w + \bar{a}_l R \beta_L\right)\overline{q_t' \phi'}$$

The buoyancy parameters $\bar{\beta}_T$ and $\bar{\beta}_w$ introduced in (2.2.15) are thus seen to be

$$\bar{\beta}_T = \beta_T - \bar{a}_l \bar{b}_l R \beta_L$$
$$\bar{\beta}_w = \beta_w + \bar{a}_l R \beta_L \qquad (3.1.15)$$

The assumption expressed in (2.2.20) is equivalent to the hypothesis

$$\overline{\phi'\psi'q_l'} = (\overline{\phi'\psi's'})(\overline{s'q_l'}/\sigma_s^2) = \bar{a}_l R(\overline{\phi'\psi'q_t'} - \bar{b}_l \overline{\phi'\psi'\theta_l'}) \qquad (3.1.16)$$

For diagnostic purposes it may be useful to have formulae for the vertical turbulent fluxes of θ, q and q_l, these are not required in the scheme to calculate anything. In terms of the parameter R the formulae are

$$\overline{w'\theta'} = \left(1 - \frac{L}{c_p \Pi} \bar{a}_l \bar{b}_l R\right)\overline{w'\theta_l'} + \frac{L}{c_p \Pi} \bar{a}_l R \, \overline{w'q_t'} \qquad (3.1.17)$$

$$\overline{w'q'} = (1 - \bar{a}_l R)\overline{w'q_t'} + \bar{a}_l \bar{b}_l R \, \overline{w'\theta_l'} \qquad (3.1.18)$$

$$\overline{w'q_l'} = \bar{a}_l R(\overline{w'q_t'} - \bar{b}_l \overline{w'\theta_l'}) \qquad (3.1.19)$$

The liquid water variance is

$$\overline{q_l'^2} = \bar{q}_l(\sigma_s Q_1 - \bar{q}_l) + \sigma_s^2 R \qquad (3.1.20)$$

If (3.1.13a) is used in preference to (3.1.13) then R should also be replaced by C in (3.1.15) - (3.1.19). However, the factor R in (3.1.20) does not depend on hypothesis (3.1.13) and so it should be retained even if (3.1.13a) is used. The dependence of $\bar{q}_l$, $\bar{\beta}_T$ and $\bar{\beta}_w$ on $\overline{\theta_l'^2}$, $\overline{\theta_l'q_t'}$ and $\overline{q_t'^2}$ is seen to be through the variance σ_s^2.

The following relations, derived from (3.1.10), (3.1.11) and (3.1.14) will be useful in th next section where expressions for C , $\bar{q}_L$ and R are derived from specific p.d.f's:

$$\frac{\partial C}{\partial Q_1} = G(-Q_1) \qquad (3.1.21)$$

$$\frac{\partial(\bar{q}_L/\sigma_s)}{\partial Q_1} = C \qquad (3.1.22)$$

$$\frac{\partial R}{\partial Q_1} = \frac{\bar{q}_L}{\sigma_s} - C Q_1 \qquad (3.1.23)$$

These follow from the rule for differentiating an integral with variable limits:

$$\text{if} \quad F(x) = \int_{-x}^{\infty} f(x,t)\,dt \quad \text{then} \quad \frac{\partial F}{\partial x} = f(-x,t) + \int_{-x}^{\infty} \frac{\partial f}{\partial x}\,dt .$$

3.2 Some simple p.d.f's and associated formulae for C, q_L and R

Sommeria and Deardorff (1977) and Mellor (1977) considered a Gaussian form for the p.d.f.

$$G(t) = \frac{1}{\sqrt{2\pi}} e^{-t^2/2}$$

This has the properties:

$$\int_{-\infty}^{\infty} G(t)\,dt = 1 , \quad \int_{-\infty}^{\infty} t\,G(t)\,dt = 0 , \quad \int_{-\infty}^{\infty} t^2 G(t)\,dt = 1 , \quad \int_{-\infty}^{\infty} t^3 G(t)\,dt = 0 .$$

The last result states that the skewness is zero. This form for G is analytically integrable to obtain formulae for C, $\bar{q}_L$ and R in terms of exponential and error functions:

$$C = \tfrac{1}{2}\left[1 + \operatorname{erf}\left(\frac{Q_1}{\sqrt{2}}\right)\right] , \quad \frac{\bar{q}_L}{\sigma_s} = C Q_1 + \frac{1}{\sqrt{2\pi}} e^{-Q_1^2/2} , \quad R = C .$$

These forms are expensive to compute and so alternative p.d.f's have been sought which give simpler functions for C, $\bar{q}_i$ and R in terms of Q_1 and σ_s .

A very simple "top hat" p.d.f. is:

$$G(t) = \begin{cases} 0 & t \leq -a \\ 1/2a & -a < t < a \\ 0 & a \leq t \end{cases} \qquad (3.2.1)$$

This satisfies $\int_{-\infty}^{\infty} G = 1$, $\int_{-\infty}^{\infty} t\,G = 0$ and $\int_{-\infty}^{\infty} t^2 G = 1$ if $a = \sqrt{3} = 1{\cdot}7321$. The distribution has zero skewness like the Gaussian. The corresponding formulae for C, $\bar{q}_i$ and R can be shown to be

$$C = \begin{cases} 0 & Q_1 \leq -\sqrt{3} \\ \frac{1}{2}(1 + Q_1/\sqrt{3}) & -\sqrt{3} < Q_1 < \sqrt{3} \\ 1 & \sqrt{3} \leq Q_1 \end{cases} \qquad (3.2.2)$$

$$\bar{q}_i = \begin{cases} 0 & Q_1 \leq -\sqrt{3} \\ \sqrt{3}\,\sigma_s C^2 & -\sqrt{3} < Q_1 < \sqrt{3} \\ \sigma_s Q_1 & \sqrt{3} \leq Q_1 \end{cases} \qquad (3.2.3)$$

$$R = \begin{cases} 0 & Q_1 \leq -\sqrt{3} \\ C^2(2 - Q_1/\sqrt{3}) & -\sqrt{3} < Q_1 < \sqrt{3} \\ 1 & \sqrt{3} \leq Q_1 \end{cases} \qquad (3.2.4)$$

These functions are shown in figure 1. Unlike the Gaussian this p.d.f does not give R=C but the difference between the two curves is small. The gradient $\partial C/\partial Q_1$ is discontinuous at $Q_1 = \pm\sqrt{3}$ since G is discontinuous at $t = \mp\sqrt{3}$ (see relation 3.1.21), and $\partial C/\partial Q_1 = 1/2\sqrt{3} = 0{\cdot}2887$ at $Q_1 = 0$ as compared with $1/\sqrt{2\pi} = 0{\cdot}3989$ for the Gaussian p.d.f.

A better simple approximation to the Gaussian is the piecewise linear 'triangular' p.d.f.

$$G(t) = \begin{cases} 0 & t \leq -a \\ \frac{1}{a}(1 + t/a) & -a < t < 0 \\ \frac{1}{a}(1 - t/a) & 0 \leq t < a \\ 0 & a \leq t \end{cases} \qquad (3.2.5)$$

$\int_{-\infty}^{\infty} t^2 G = 1 \Rightarrow a = \sqrt{6} = 2.449$ and again the distribution has zero skewness. This p.d.f gives:

$$C = \begin{cases} 0 & Q_1 \leq -\sqrt{6} \\ \frac{1}{2}(1 + Q_1/\sqrt{6})^2 & -\sqrt{6} < Q_1 \leq 0 \\ 1 - \frac{1}{2}(1 - Q_1/\sqrt{6})^2 & 0 < Q_1 < \sqrt{6} \\ 1 & \sqrt{6} \leq Q_1 \end{cases} \qquad (3.2.6)$$

$$\bar{q}_1 = \begin{cases} 0 & Q_1 \leq -\sqrt{6} \\ \frac{\sigma_s}{\sqrt{6}}(1 + Q_1/\sqrt{6})^3 & -\sqrt{6} < Q_1 \leq 0 \\ \sigma_s Q_1 + \frac{\sigma_s}{\sqrt{6}}(1 - Q_1/\sqrt{6})^3 & 0 < Q_1 < \sqrt{6} \\ \sigma_s Q_1 & \sqrt{6} \leq Q_1 \end{cases} \qquad (3.2.7)$$

$$R = \begin{cases} 0 & Q_1 \leq -\sqrt{6} \\ \frac{1}{2}(1 + Q_1/\sqrt{6})^3 (1 - Q_1/\sqrt{6}) & -\sqrt{6} < Q_1 \leq 0 \\ 1 - \frac{1}{2}(1 - Q_1/\sqrt{6})^3 (1 + Q_1/\sqrt{6}) & 0 < Q_1 < \sqrt{6} \\ 1 & \sqrt{6} \leq Q_1 \end{cases} \qquad (3.2.8)$$

Figure 2 illustrates these functions. The difference between R and C is very small: this indicates that this p.d.f. is a good approximation to the Gaussian. Also $\partial C/\partial Q_1 = 1/\sqrt{6} = 0.4082$ at $Q_1 = 0$ as compared to the value 0.3989 for the Gaussian. The gradient $\partial C/\partial Q_1$ is continuous for this p.d.f.

ALthough the triangular p.d.f represents the Gaussian better than the top-hat p.d.f. it is more complicated (there are four regions on the Q_1 axis to consider and higher order polynomials in Q_1 to evaluate). Results from the limited number of tests done so far are not very sensitive to the p.d.f. chosen. The simpler top-hat p.d.f. is therefore recommended for the mesoscale model.

It has been pointed out by Bougeault (1981 a and b, 1982) that the choice of a p.d.f. with zero skewness may not be realistic. The skewness of G is

$$A \equiv \int_{-\infty}^{\infty} t^3 G(t)\, dt = \frac{\overline{s'^3}}{\sigma_s^3}$$

Now $\overline{s'^3}$ is given by

$$\overline{s'^3} = \bar{a}_l^3 \left(\overline{q_t'^3} - 3\bar{b}_l \overline{q_t'^2 \theta_l'} + 3\bar{b}_l^2 \overline{q_t' \theta_l'^2} - \bar{b}_l^3 \overline{\theta_l'^3} \right) \qquad (3.2.9)$$

and is in principle computable from the turbulence scheme. A positive skewness will allow, for a given σ_s, initiation of condensation at a lower mean relative humidity. Correct representation of scattered cumuli or the undulating tops and bottoms of stratiform cloud may need therefore a p.d.f with non-zero skewness. Further work is required to find a computationally simple skew p.d.f.

4. COMPUTATIONAL DETAILS

4.1 The calculation of the static stability parameter N^2 presents a problem since it is not explicitly defined by (2.2.19). The buoyancy parameters $\bar{\beta}_T$ and $\bar{\beta}_w$ depend on the quantities $\overline{\theta_l'^2}$, $\overline{\theta_l' q_t'}$ and $\overline{q_t'^2}$ (and possibly higher order quantities); these in turn, through the quantity $\tau_3 K_h$ depend on N^2. Obtaining an explicit formula for N^2 out of this complex chain of nonlinear dependencies would be very difficult and the result would not be suitable for computational purposes.

In a simple one-dimensional model, where storage space for variables is not a constraint, the obvious solution to the problem is to carry over a suitable quantity or quantities from the previous time level. Since it is $\bar{q}_l$ and R (or C if (3.1.13a) is used) which are required in the calculation of the buoyancy parameters, carrying over these two quantities minimises computation. For a p.d.f. with zero skewness only one quantity, σ_s, need strictly be carried over since C, $\bar{q}_l$ and R can then be derived. However, for a skew p.d.f. the skewness, A, is also required. Since C and $\bar{q}_l$ are the more physically meaningful quantities and are used directly in calculations, they are stored from one time level to the next in the 1-d model.

In the full 3-d mesoscale model $\bar{q}_l$, $\bar{q}$ and $\bar{\theta}$ are already available from previous time levels. However, the only available variable characterising the turbulence is the t.k.e. The quantity $l^2 N^2$ is estimated by a reverse application of the diagnostic t.k.e. equation. This gives:

$$l^2N^2 = \frac{(F_2 E_{neut} - F_{10}\bar{E}) + \sqrt{(F_2 E_{neut} - F_{10}\bar{E})^2 - 4F_{11}\bar{E}(\bar{E} - E_{neut})}}{2F_{11}}$$

Since the t.k.e. will have been calculated from its prognostic equation involving turbulent transports this value of l^2N^2 will not be precise. It is only used in the calculation of the buoyancy parameters $\bar{\beta}_{T,W}$ after which a truer value can be calculated from (2.2.19) and subsequently used.

4.2 A similar type of problem exists in calculating the surface static stability N^2_{surf} from (2.3.16), even after the buoyancy parameters have been calculated. Equation (2.3.16) involves the surface moisture availability parameter $\alpha = 1/(1 + C_H|V_1|r_s)$. Unless $r_s = 0$ this depends on C_H which is in turn a function of stability. Again an explicit formula is difficult to find and would be useless for practical purposes. In the 1-d model α is carried over from the previous time level. It is proposed that in the mesoscale model C_H is replaced by its neutral value of $k^2/(\log z_1/z_0)^2$ in the calculation of α for use in (2.3.16). This then allows a full stability dependent C_H to be found for calculating fluxes.

4.3 As with the moist scheme described in (I) there is the possibility of the effective diffusion coefficients for the thermodynamic and moisture variables being negative. The same physically artificial and unjustifiable but effective procedure as in (I) is used to limit the values of N_T^2 and N_q^2 These quantities are given by:

$$N_T^2 = \bar{\beta}_T \frac{\partial \bar{\theta}_L}{\partial z} \quad , \quad N_q^2 = \bar{\beta}_W \frac{\partial \bar{q}_t}{\partial z}$$

in the wet scheme.

5. TESTS OF THE SCHEME IN A 1-D MODEL

5.1 Wangara day 33 with zero surface resistance to evaporation

The first test of the scheme was carried out with the data for Wangara day 33 as used in tests of the moist scheme in (I). The 1-d model with gridpoints at 10, 100, 300, 500, 700, 900, 1100, 1300, 1500, 1700 and 2000m

was used. The results were almost identical to those produced by the moist scheme. This is as it should be since no clouds formed in reality or the model. In order to artificially induce cloud the surface resistance to evaporation was then set to zero rather than its realistic high value. This has the effect of transforming the Wangara site from desert to swamp!

As expected this change greatly increased the latent heat and moisture fluxes from the surface at the expense of sensible heat. After 0800 hours local time fog (i.e. cloud at the bottom model level) formed and by 1000 hours this lifted to layer cloud at 100m, beneath the steadily eroding nocturnal inversion. By 1200 hours the inversion had been completely eroded allowing turbulent eddies to penetrate rapidly into the near neutral layer left over from the previous day's (dry!) mixing. The cloud fraction in this layer was $\leq 1/3$ and can be interpreted as an indication of scattered cumuli associated with the penetrating eddies. Evidence of this can be seen by comparing the θ and θ_l profiles at 1200h in figures 3 and 4. Between 300 and 700m the potential temperature is slightly greater than the conserved liquid water potential temperature. This is due to the latent heat released in the cloud. The liquid water content at 1200 hrs can be seen in figure 5(b). Its magnitude is small since the cloud cover is far from complete. The in-cloud liquid water content is about three times as large.

This scattered cumuli stage is transitory. The turbulent flux of moisture is sufficiently large to ensure the formation of a layer of stratocumulus beneath the upper inversion. By 1500 hrs a layer with cloud fraction of 0.8 has developed at 900 m. The layer beneath this level is fairly well mixed as can be seen from the profiles of the conservative variables θ_l (figure 3) and q_t (figure 5(a)) for this time. The latent heating can again be seen by comparing the θ_l and θ profiles (figures 3 and 4) and the liquid water content is clearly evident in figure 5(b).

The normalised t.k.e. profile is shown in figure 6(a). The convective velocity $w_* = \left[\frac{g}{\theta_v}(\overline{w'\theta_v'})_{surf}.h\right]^{1/3}$ is not so appropriate for normalising the t.k.e. when there are sources other than buoyancy generated at the surface. In reality radiative cooling from the top of cloud layers is a significant

source of buoyantly generated t.k.e. The model used in this test does not have any representation of radiation except at the surface so the reservations about using w_* are not so great. There is, however, a source of t.k.e. at cloud top evident in this simulation which is due to the "cloud top entrainment instability" (Deardorff (1980) and Randall (1980)). Figure 6(a) shows a level of turbulence at the top of the mixed layer exceeding that of simulations of cloud-free layers. This is a result of the positive buoyancy flux at this level (figure 6(b)). The generation of positive buoyancy by the entrainment at the top of cloudy mixed layers is in sharp contrast to the behaviour of cloud free layers. Although the air entrained from the free atmosphere is potentially warmer it is also much drier. A pocket of this entrained air therefore cools because liquid water in the cloud evaporates into it. The criterion for this process to be a source of t.k.e. is given by Randall (1980) to be

$$\beta \Delta\theta_e < \theta \Delta q_t$$

where Δ represents the jump in a variable across the inversion layer and β is a slowly varying function of temperature of magnitude $\simeq 1/2$. The relatively high level of t.k.e. at the inversion leads to entrainment fluxes larger than those of cloud-free layers. The fluxes of θ_l and q_t are shown in figures 6(b) and 7 for 1500 hrs. Owing to the entrainment the mixed layer grows and by 1800 hrs has reached 1100m in height with a solid deck of stratocumulus at the top.

These results, although artificial and obtained from a model without radiative or precipitation physics, show realistic behaviour. In particular, the maintenance of t.k.e. in cloudy layers and enhanced entrainment at cloud top are well simulated.

5.2 Marine stratocumulus simulation

As a further test the 1-d model with the same resolution was used to simulate the development of a layer of stratocumulus over sea. The sea surface temperature was held constant at 18 °C. The initial potential temperature profile was set to $(18 + \gamma_c z)$ °C up to 1500m with $\gamma_c = 0{\cdot}3$ °K km^{-1},

with a stable layer above. The initial specific humidity was constant up to 1500m with a value of 6 g kg^{-1}. This gives a relative humidity of just 100% at 1500m. The initial θ profile (which is the same as the initial θ_l profile since there is no liquid water) is shown in figure 8 and figure 12 shows the initial relative humidity profile. These initial conditions represent a well mixed cloud-free boundary layer 1.5 km deep on the point of becoming cloudy.

The model was run for 144 hours, i.e. 6 days. Throughout the simulation there is very little turbulent flux of θ_l as the boundary layer is in thermal equilibrium with the sea surface. The flux of moisture from the sea steadily increases the humidity of the mixing layer (figures 10(a) and 12). Figure 10(b) shows the development of a stratocumulus layer. For the first four days the layer deepens by a steady lowering of the cloud base to a little above 700 m. During this period the turbulence in the boundary layer is leading to entrainment at cloud top. The effect of the entrainment can be seen from the reduction in θ_l and increase in q_l at 1700m (see figures 8 and 10(a); t.k.e. profiles are shown in figure 11). During the remaining two days of the simulation the inversion is further eroded and the cloud top rises to 1700m. During this process the cloud base is prevented from becoming lower as the water substance is required to form the cloud in the layer 1500-1700m.

The latent heat released during cloud formation shows in the wet adiabatic lapse rate for θ in the cloud layer in figure 9. The stability, in this wet scheme, depends on the gradients of the conservative variables θ_l and q_l and so the positive gradient in θ in the cloud does not inhibit turbulence as it would in a dry scheme.

An interesting feature of the profiles for T+5 and T+6 days is that the cloud and sub-cloud layer seem to have become detached. This is clearly evident in the t.k.e. profiles; at T+6 days the t.k.e. falls to its minimum value at 500m. The reason appears to be that the rapid entrainment due to the cloud top entrainment instability mixes warmer air (in the sense of greater θ_l) into the boundary layer. This is mixed right down to the sub-cloud layer which therefore becomes slightly stable. The T+6 days θ_l

profile (figure 8) shows this effect. Figure 10(a) shows the development of a distinct hydrolapse below cloud base in association with this separation of layers.

The liquid water content of the upper parts of the cloud would in reality be prevented from becoming so large by the formation and precipitation of rain drops. A parametrization of this process is not yet in the 1-d model but tests of the wet turbulence scheme in the 3-d mesoscale model will provide an opportunity to see how the precipitation physics and the turbulence interact. The development of the stratocumulus would be faster if a parametrization of the longwave cloud top cooling was included. With these extra processes included in the model a realistic simulation of the break-up of a stratocumulus layer may be possible.

τὰ πάντα ἐν Χριστῷ συνέστηκεν

REFERENCES

Bougeault P, (1981a)

Modelling the trade-wind cumulus boundary layer.

Part I: Testing the ensemble cloud relations against numerical data.

J. Atmos. Sci. 38, 2414-2428.

Bougeault P, (1981b)

Modelling the trade-wind cumulus boundary layer.

Part II: A high order one dimensional model.

J. Atmos. Sci. 38, 2429-2439.

Bougeault P, (1982)

Cloud ensemble relations for use in higher order models of the p.b.l.

J. Atmos. Sci. 39, 2691-2700.

Deardorff J W (1980)

Cloud top entrainment instability. J. Atmos. Sci 37, 131.

Machin N A (1983)

A stratiform condensation scheme for the UKMO mesoscale model.

Met O 11 Technical Note NO 167.

Mellor G L (1977)

The Gaussian Cloud Model Relations. J. Atmos. Sci. 34, 356-358 and 1483-1484.

Randall D A (1980)

Conditional instability of the first kind, upside-down.

J. Atmos. Sci. 37, 125-130.

Sommeria G and Deardorff J W (1977)

Subgrid-scale condensation in models of non-precipitating clouds.

J. Atmos. Sci. 34, 344-355.

E.R.

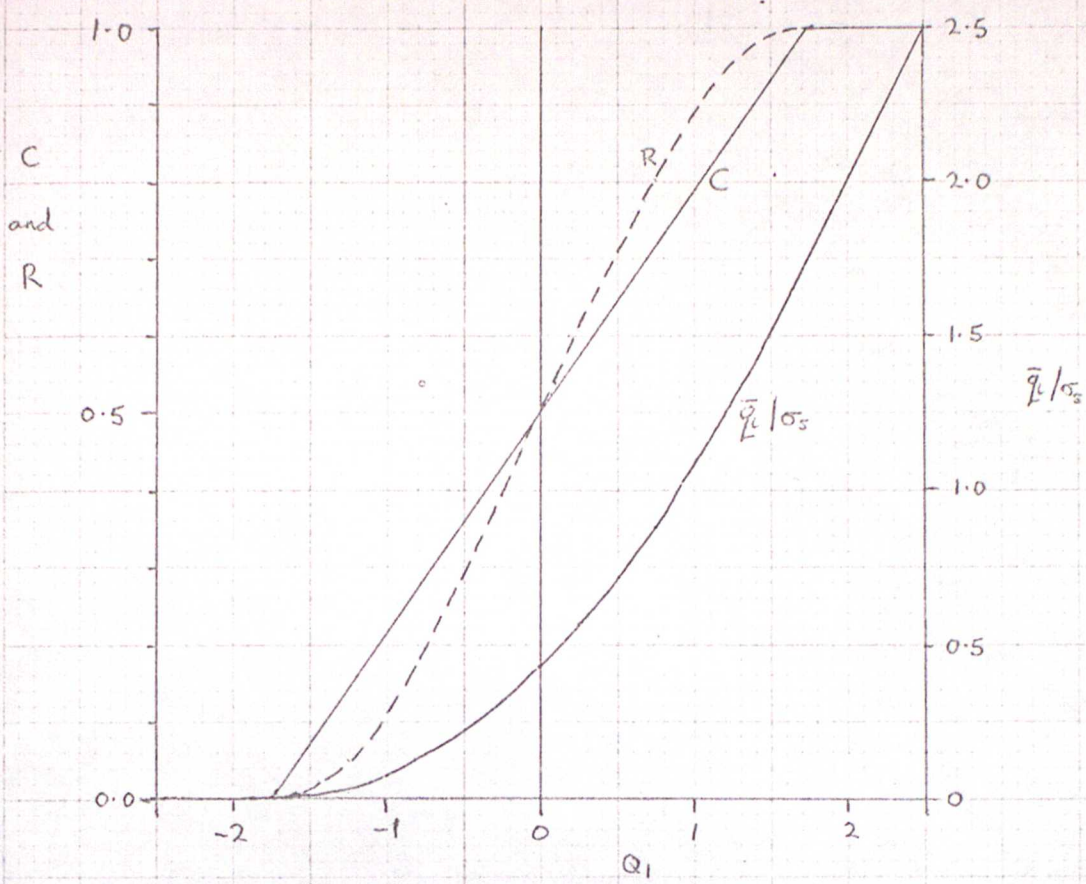

FIGURE 1 C, q_L and R derived from "top hat" p.d.f.

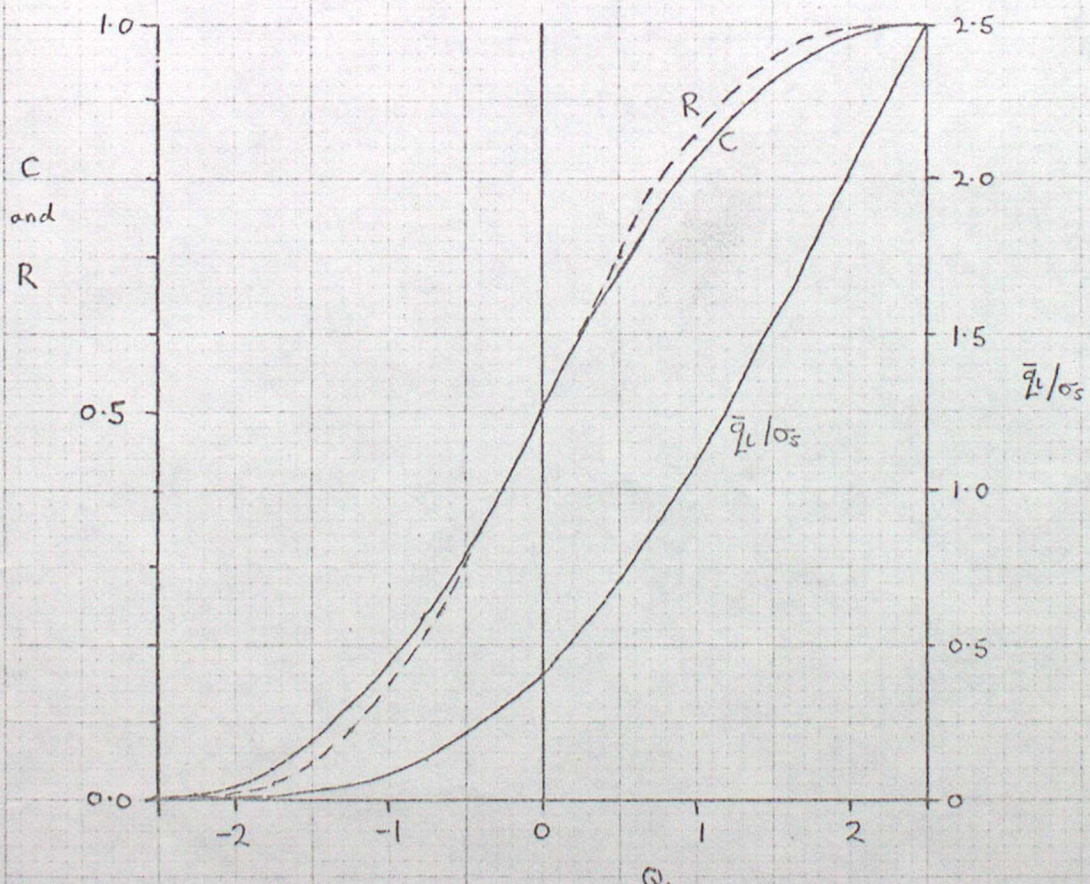

FIGURE 2. C, q_L and R derived from "triangular" p.d.f.

FIGURE 3. θ_l PROFILES "WET WANGARA DAY 33"

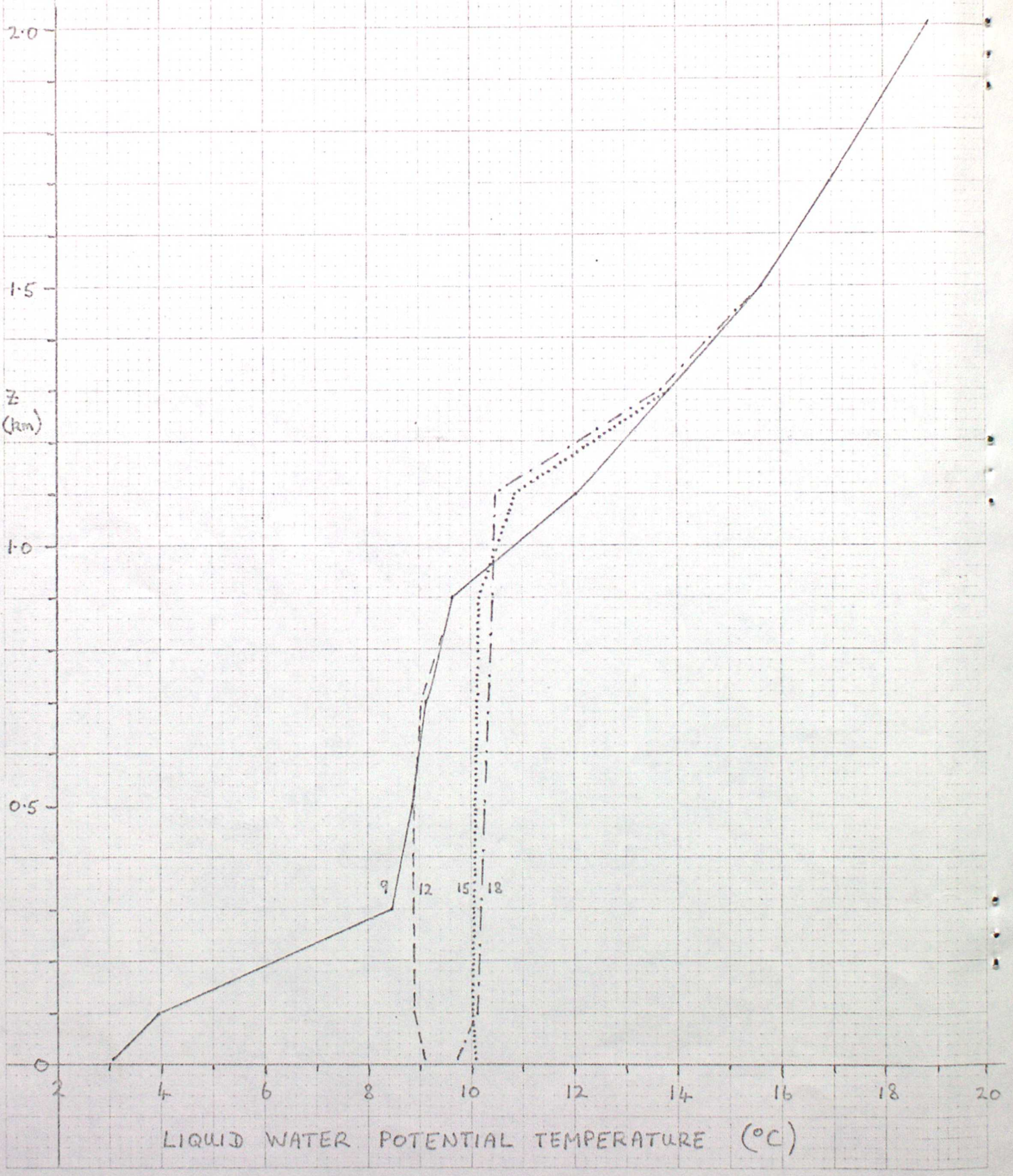

FIGURE 4. θ PROFILES "WET WANGARA DAY 33"

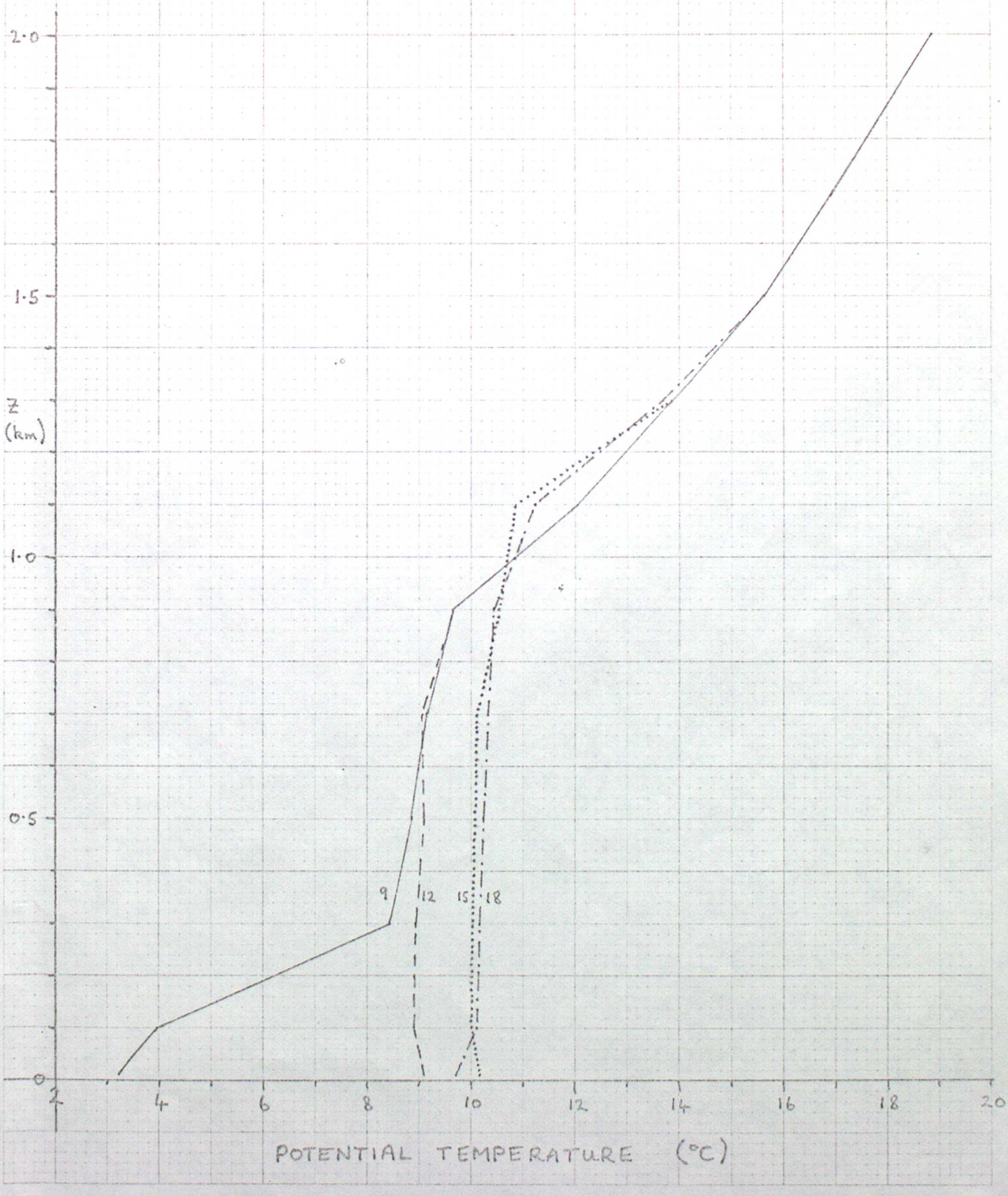

FIGURE 5. SPECIFIC TOTAL WATER AND LIQUID WATER CONTENT PROFILES "WET WANGARA DAY 33"

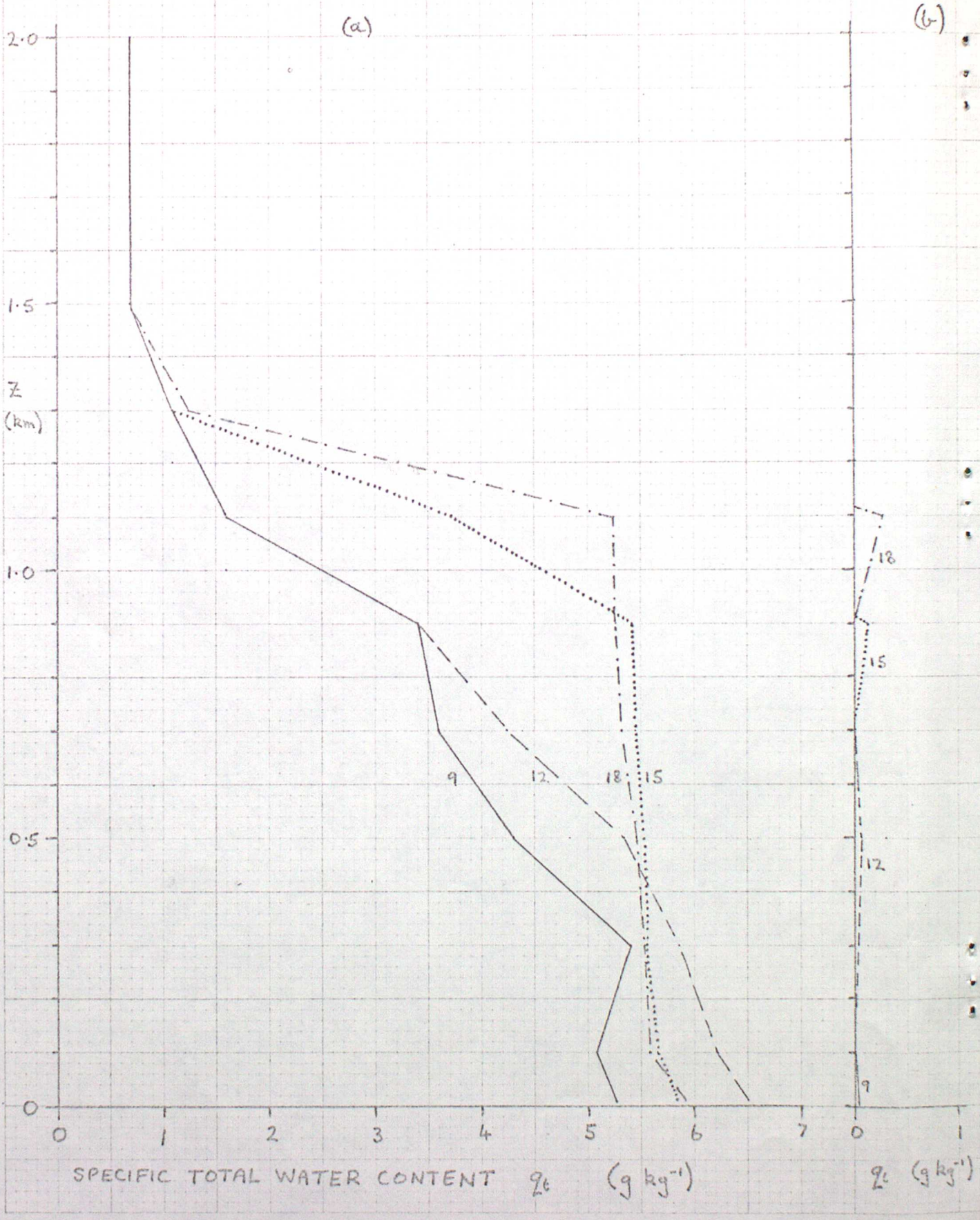

FIGURE 6. NORMALISED T.K.E., THETAL FLUX AND BUOYANCY FLUX AT 15.00 hr LT "WET WANGARA DAY 33"

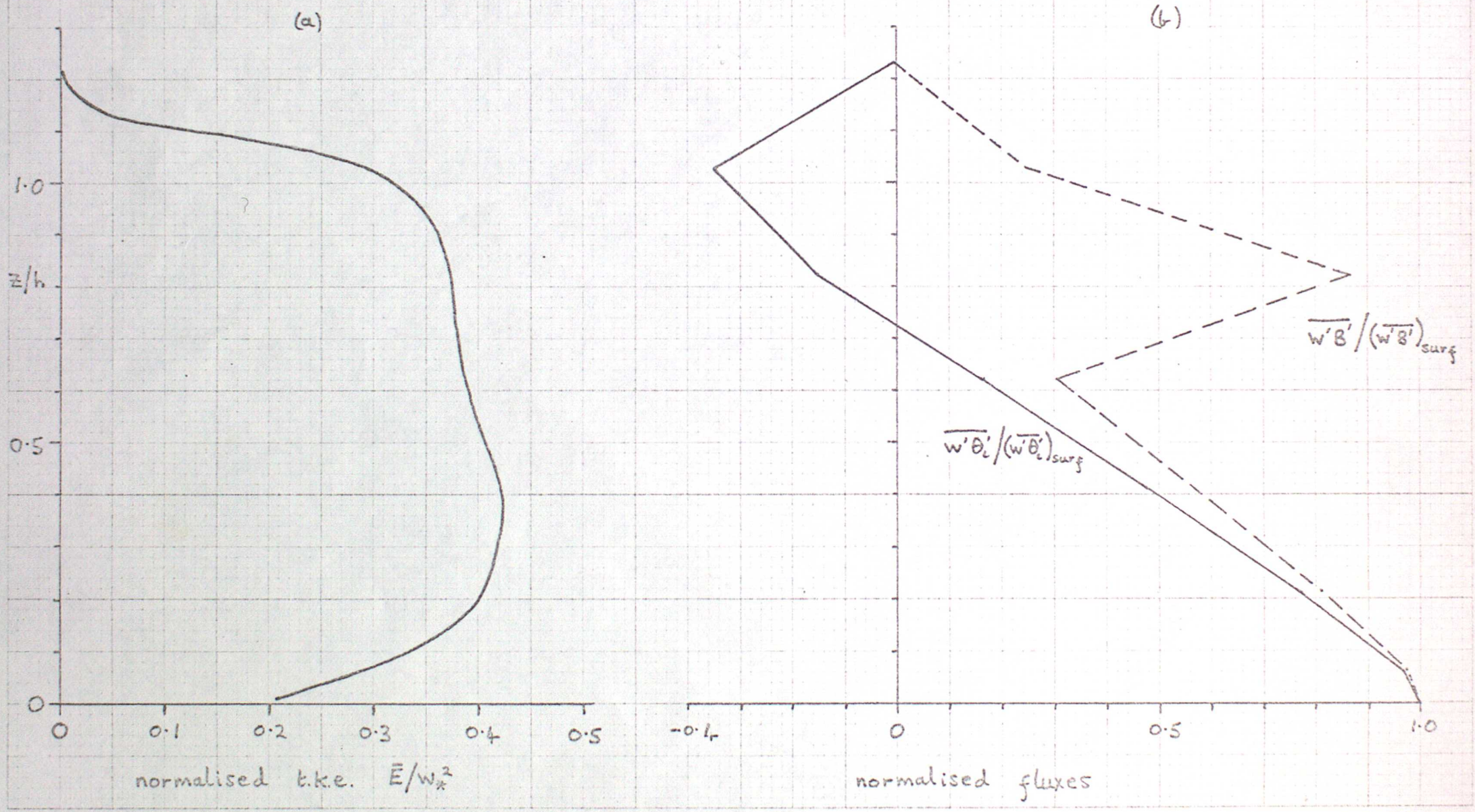

FIGURE 7. NORMALISED TOTAL WATER FLUX

AT 15.00 hr LT "WET WANGARA DAY 33"

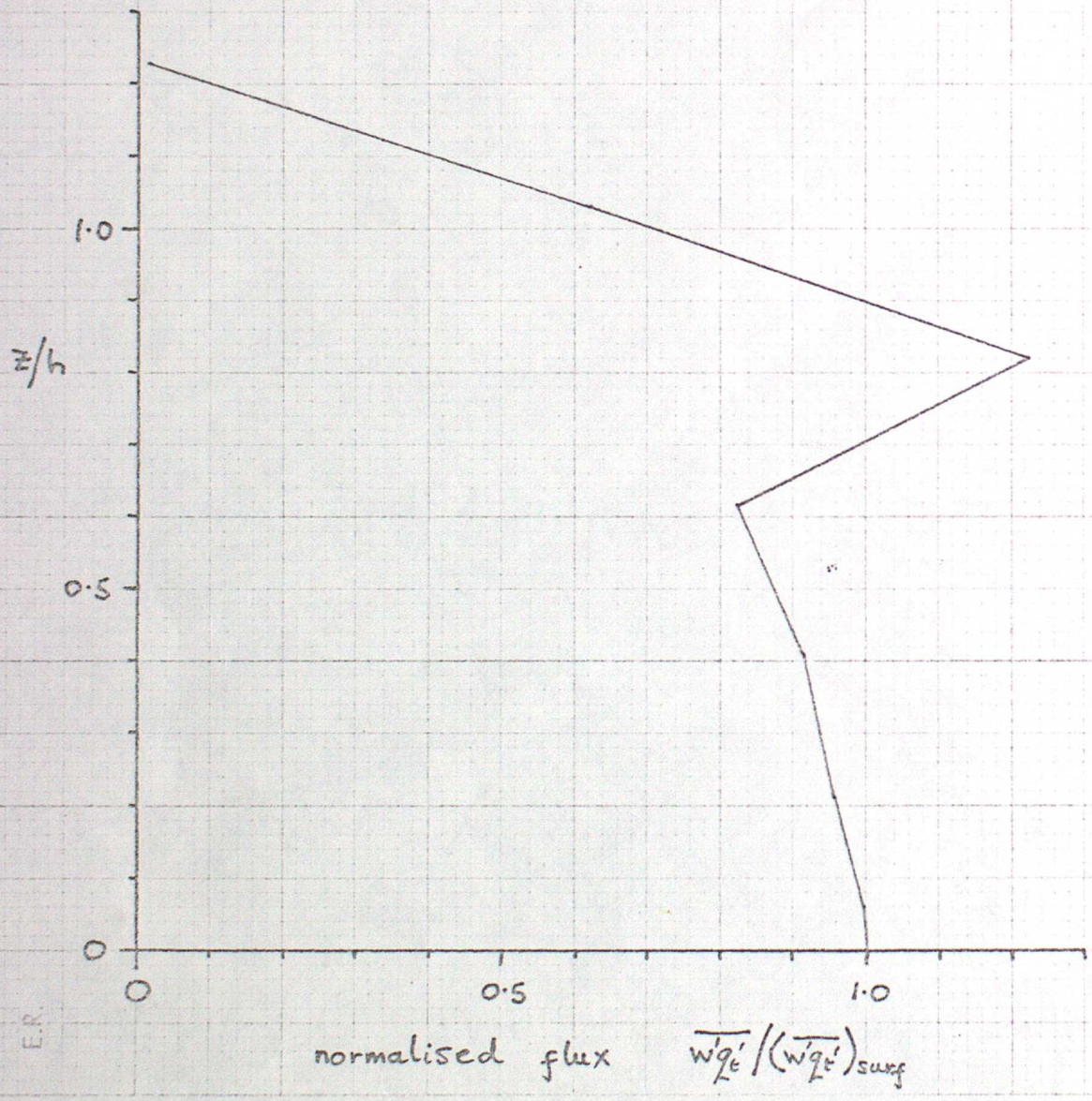

E.R.

FIGURE 8. LIQUID WATER POTENTIAL TEMPERATURE PROFILES

MARINE Sc

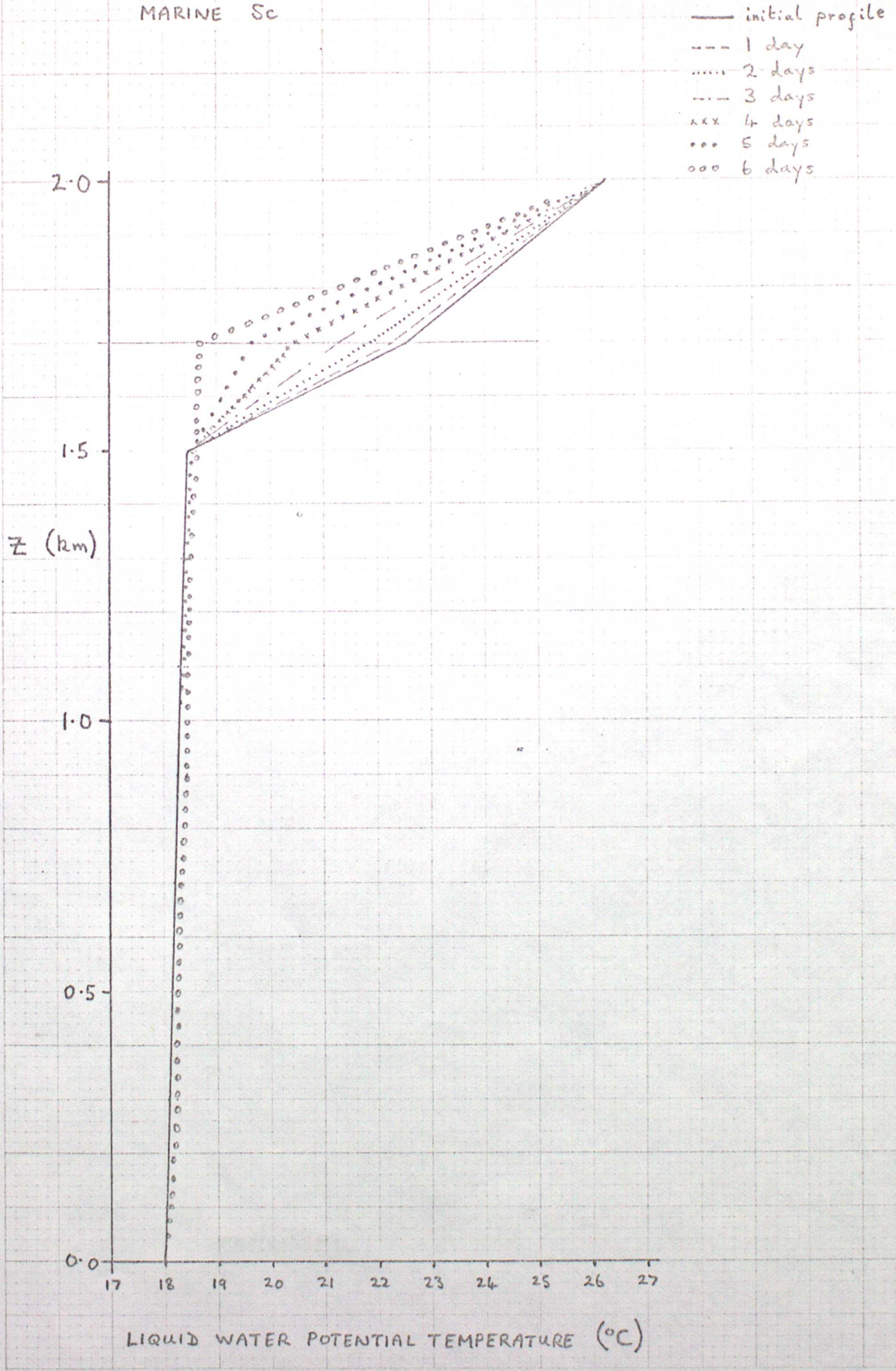

E.R.

FIGURE 9. POTENTIAL TEMPERATURE PROFILES

MARINE Sc

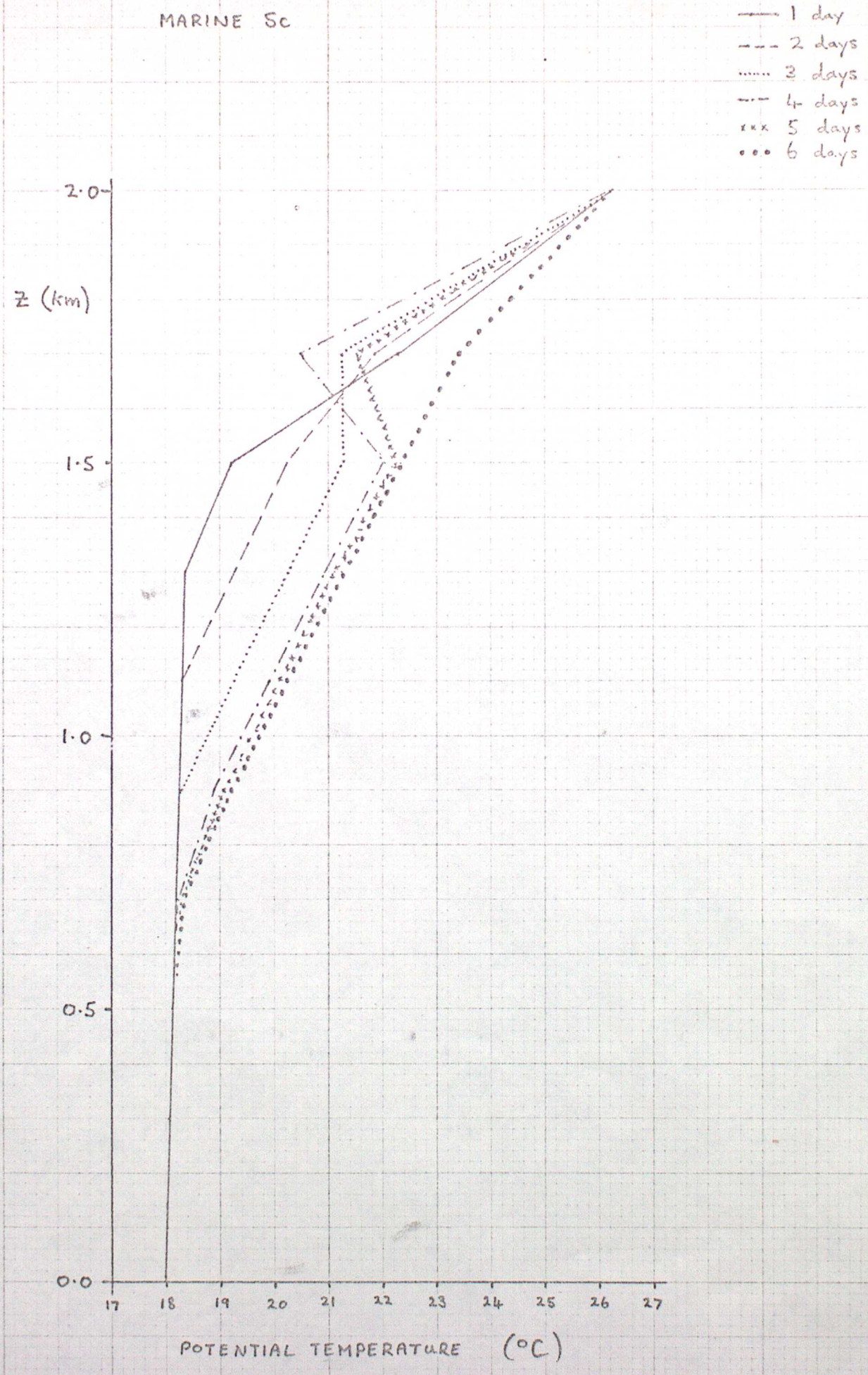

E.R.

FIGURE 10. SPECIFIC HUMIDITY AND LIQUID WATER CONTENT PROFILES, MARINE Sc

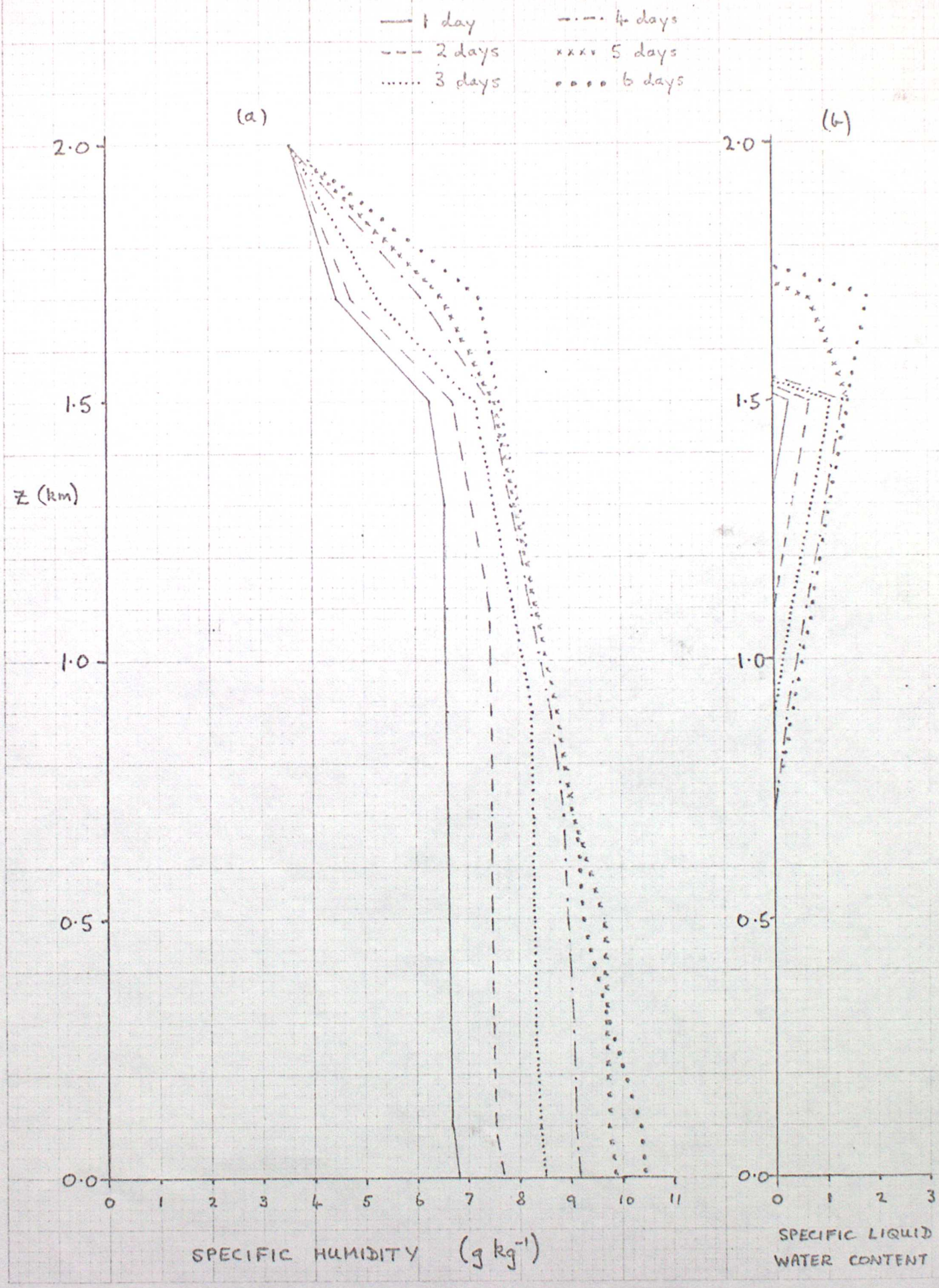

FIGURE 11. T.K.E PROFILES, MARINE Sc

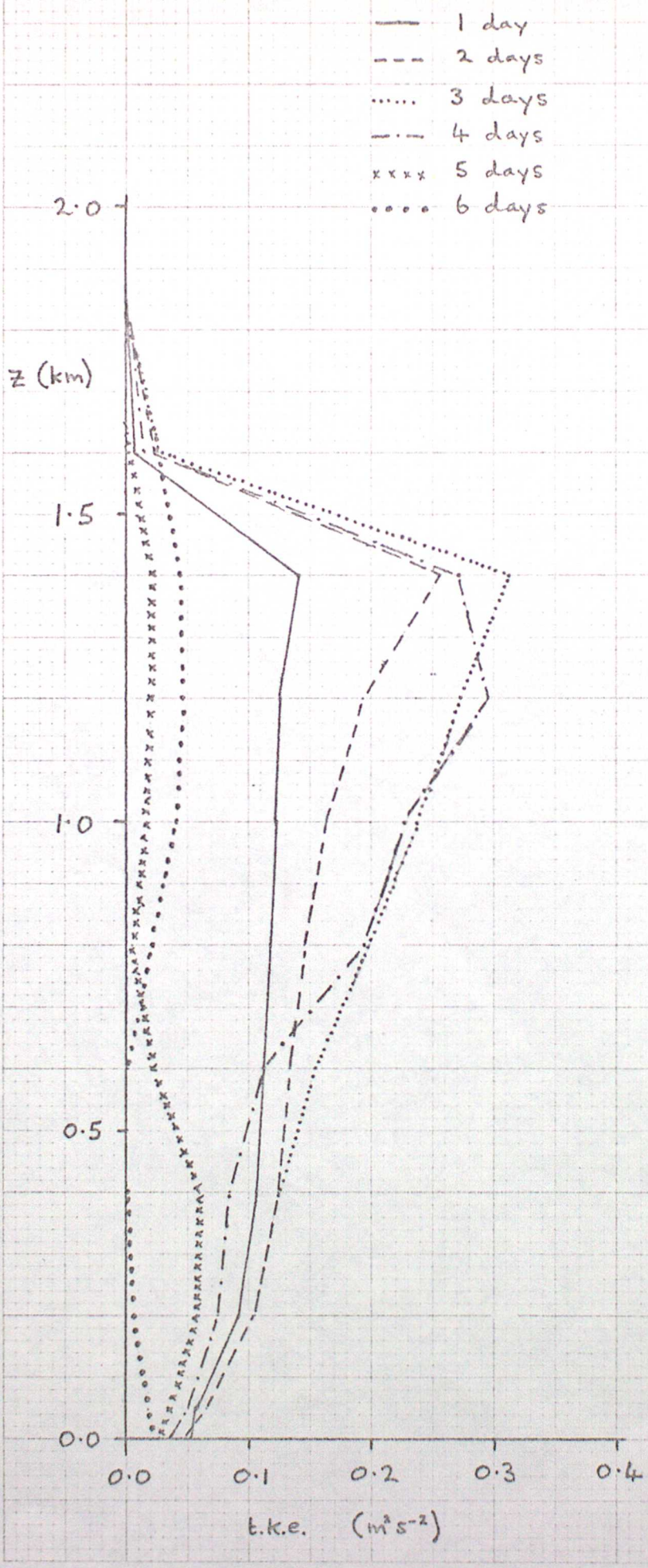

E.R.

FIGURE 12. RELATIVE HUMIDITY PROFILES

MARINE Sc